Neurite Density Measured in Human Subject using Hybrid Diffusion Imaging

Shiyang Wang[1,2], Michael Chopp[1,2], Siamak Pourabdollah Nejad D. [1], JiaNi Hu[3], and Quan Jiang[1,2]

[1]*Neurology, Henry Ford Hospital, Detroit, MI, United States,* [2]*Physics, Oakland University, Rochester, MI, United States,* [3]*Radiology, Wayne State University, Detroit, MI, United States*

Abstract: Neurite density measurement was performed on human subjects. Simultaneous image refocusing sequence (SIR) combined with hybrid diffusion gradient encoding scheme (HYDI) was used in patient with traumatic brain injury (TBI).

Introduction: Neurorestorative therapy which induces neurite outgrowth improves functional recovery in experimental TBI, [1]. MRI neurite density significant increases in MSC treated group animals is observed [2]. To date, no MRI measurement of neurite density after TBI had been investigated in human subjects. In this study, we tested the feasibility of HYDI-SIR sequence in measuring human neurite density. We report for the first time that quantitative MRI neurite density can monitor the patient neurological changes after TBI.

Methods: Five Healthy volunteers, average age 34.6 years old were scanned in GE Signa 3T system using PGSE sequence with hybrid gradient encoding [3], b-max=9000 s/ mm^2, matrix size 256x256, 25 slices, TR/TE=10000/143.6 ms, number of average=1, total scan duration 23 minutes. TBI patient data was acquired two month after traumatic incidence. Patient scan was performed in Siemens TrioTim 3T scanner using SIR sequence with the gradient encoding scheme same as healthy volunteers, with b-max=8000s/mm^2, matrix size 128x128, fifteen slices with 4 mm thickness, TR/TE=3027/65 ms, number of average=1, scan time is approximately 11 minutes.

Data fitting procedure is the same as in [2]. Image data from the 3rd shell of 21 gradient directions with a b-value of 1500 s/mm^2 is used for visualization of fiber crossings and fiber tracking of human subject data. Image data from all shells was used to calculate maximum orientation distribution function (ODF) and principal diffusion directions were extracted from max-ODFs. Neurite density values were measured in gray matter, putamen, Thalamus, corpus callosum, frontal white matter, and internal capsule regions. Human brain autopsy tissue samples were studied for axonal density analysis. Axonal density and orientation were examined using a combined Nissl/silver-staining method. Double Bielschowsky and Luxol fast blue staining was used to demonstrate axons and myelin, respectively. **Results:** Neurite densities exhibited a significant correlation (r^2>0.91, p<0.001) between MRI and immuno-histochemistry measurements of healthy subjects (Figure 1). TBI patient shows neurite density increased in lesion boundary regions (occipital lobe) and decreased in core lesion region. ADC map shows slightly increased diffusion coefficient value around lesion boundary areas (Figure 2).

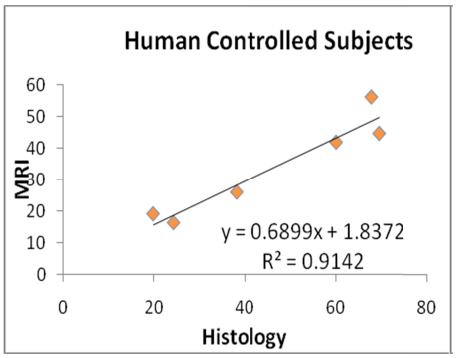

Figure 1 Correlation of MRI Neurite Density with Histological Staining Result.

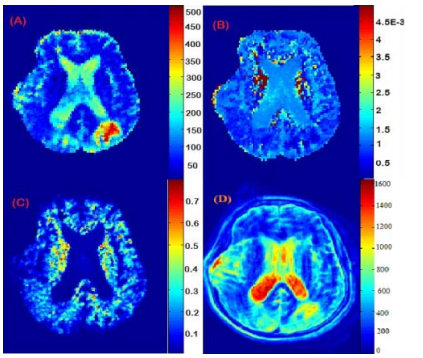

Figure 2 Neurite Density Measured from TBI patient. Original image (b=0) (A), effective diffusion coefficient (B), neurite density (C), T2 weighted image (D).

Discussion and Conclusion: SIR sequence combined with hybrid diffusion encoding scheme provide an effective imaging method to measure neurite density with acceptable scan duration for clinical applications. This method provides a non-invasive approach to directly quantify neurite density in human subjects. High correlations were detected between MRI and histological neurite densities in healthy human subject. Increased neurite density is observed in TBI lesion boundary regions mainly due to tissue self-repair low neurite density values in lesion core region may caused by tissue necrosis. This method provides an effective approach to dynamically monitor the progress of axonal remodeling after TBI. And it could be potentially applied to not only TBI recovery but to other neurological diseases, such as stroke, hemorrhage, and neurodegenerative diseases.

References:

[1] Li Y, Chopp M. *Neurosci Lett*. 456:120 (2009).
[2] Wang S, Proc. Intl. Soc. Mag. Reson. Med. (2011).
[3] Wu Y.C. NeuroImage 36(3):617-629 (2007).
[4] Jespersen S.N., NeuroImage 34:1473 (2007).

Grant support: Supported by NINDS grants P50 NS23393, PO1 NS42345, RO1 NS064134, RO1 NS48349, and HL64766.